Journal of Applied Physics

Enhanced co-deformation of a heterogeneous nanolayered Cu/Ni composite

Cite as: J. Appl. Phys. **126**, 215111 (2019); https://doi.org/10.1063/1.5121625
Submitted: 30 July 2019 . Accepted: 18 November 2019 . Published Online: 04 December 2019

Yaodong Wang, Jianjun Li, Wenjun Lu, Fuping Yuan, and Xiaolei Wu

Journal of Applied Physics ARTICLE scitation.org/journal/jap

Enhanced co-deformation of a heterogeneous nanolayered Cu/Ni composite

Cite as: J. Appl. Phys. **126**, 215111 (2019); doi: 10.1063/1.5121625
Submitted: 30 July 2019 · Accepted: 18 November 2019 ·
Published Online: 4 December 2019

Yaodong Wang,[1] Jianjun Li,[1,2,a)] Wenjun Lu,[3] Fuping Yuan,[4] and Xiaolei Wu[4]

AFFILIATIONS

[1]School of Mechanical and Electrical Engineering, Central South University, Changsha 410083, Hunan, China
[2]State Key Laboratory of High Performance Complex Manufacturing, Central South University, Changsha 410083, Hunan, China
[3]Department of Microstructure Physics and Alloy Design, Max-Planck-Institut für Eisenforschung GmbH, Düsseldorf 40237, Germany
[4]The State Key Laboratory of Nonlinear Mechanics, Institute of Mechanics, Chinese Academy of Sciences, Beijing 100190, China

[a)]**Author to whom correspondence should be addressed:** mejjli@csu.edu.cn

ABSTRACT

Nanolayered metallic composites have attracted intensive scientific interests due to their ultrahigh strength. However, the deformation incompatibility among the component layers with high mechanical contrast leads to extremely low tensile ductility in the nanolayered composites, which is a great setback for their engineering applications. Here, by molecular dynamics simulations, we show that a heterogeneous nanolayered design by combining 2.5 nm and 24 nm Cu/Ni bilayers in a composite in an appropriate way can promote the dislocation activity of the hard phase, i.e., the Ni layers. In the new heterogeneous structure, each 24 nm Cu or Ni layer is coated on both surfaces by one 2.5 nm Cu/Ni bilayer. The simulations show that the dislocations in the 24 nm Ni layers can nucleate and glide almost synchronously with those in the 24 nm Cu layers. The enhanced dislocation activities are attributed to the presence of the 2.5 nm Cu layer that can promote the dislocation nucleation and motion in the 24 nm Ni layer by forming more nodes in the dislocation network of the interface.

I. INTRODUCTION

Many research studies show that nanolayered (NL) metallic composites possess outstanding mechanical and physical properties,[1–8] such as ultrahigh strength that approaches 1/2 or 1/3 of the theoretical limit,[9,10] due to their heterogeneous interfaces of high density. Existing investigations have been focused on the layer thickness (h) dependent strengthening mechanisms in the NL composites.[11–13] Their results show that the Hall-Petch-type strengthening[14] dominates as h is in the range of tens of nanometers to submicrometers, and that the confined layer slip of single dislocation[15] operates as h decreases below dozens of nanometers.[16–20] Although the ultrahigh strength of NLs is attractive in engineering applications, their low tensile ductility (usually less than 4% elongation[21–23]) is a great setback. The extremely low ductility results from the deformation incompatibility among the component layers with dissimilar materials that have high mechanical contrast. There are two modes of deformation incompatibility depending on layer thickness in homogeneous nanolayer structures that consist of layers with identical thicknesses: one is shear instability that occurs in very thin layers with $h < \sim 10$ nm[24–26] and the other one is strong extrusion of soft layers that appears in relatively thick layers ($h > \sim 20$ nm).[27,28] Here, the term "extrusion" is defined to describe the deformation mismatch between the constituent layers with high mechanical contrast during micropillar compression, in which the soft layer is squeezed out relative to the hard layer due to the higher deformability of the former than the latter.

There are a few efforts to alleviate the above deformation incompatibility to enhance the plasticity and ductility of NL composites by designing heterogeneous nanolayered structures, that is, the component layer thickness differs significantly.[29] For example, Wang *et al.*[30] fabricated a 5 nm Cu/35 nm amorphous CuZr NL sample by magnetron sputtering, which has a yield strength of 1.1 GPa and a tensile elongation to failure of 13.8%. They revealed that the amorphous/crystalline interface absorbs the dislocations that reach the interface, thus leading to a stable plasticity flow. Another example is a bimodal Cu/Nb NL that alternatively stacks 4 nm and 40 nm bilayers that suppresses the through thickness crack caused by shear instability in a rolling process.[31] The suppressed shear instability is due to the homogeneous dislocation slips in the 40 nm layers caused by the uniform confined layers in

the 4 nm layers. Recently, the authors[32] have investigated the deformation of a bimodal 10–100 nm Cu/Zr NL by micropillar compression that can achieve almost isostress state during deformation due to the taper of less than 2°–4° produced during fabrication of the pillars by focused ion beam billing. As compared to the isostrain state in tension and the plane strain state in rolling, the isostress state is an ideal way to test the deformation compatibility among the component dissimilar layers. The results show that the 10 nm layers enhanced the deformation compatibility among the 100 nm Cu and 100 nm Zr layers by reducing the extrusion of the 100 nm Cu layers, yet the extrusion of the Cu layers is still a big problem. Recently, we designed a new heterogeneous nanolayer Cu/Zr structure by inserting 10 nm bilayers in each 100 nm Zr–Cu or Cu–Zr interfaces. The experiments show that the extrusion of the 100 nm layers can be almost eliminated, that is, a fully compatible deformation among the Cu and Zr layers is achieved. The experimental work will be published in another article.

The aim of the heterogeneous design is to attack the general problem of deformation incompatibility (i.e., extrusion or squeezing out of the soft layer relative to the hard layer) between the soft (e.g., Cu) and hard (e.g., Ni, Zr, Cr, Nb, or amorphous CuZr) constituent layers in nanolayered structures.[3,32–35] The above-mentioned experimental investigations on Cu/Nb and Cu/Zr nanolayers show that the heterogeneous nanolayer design by combining layers with significantly different thicknesses is a promising route to improve the deformation compatibility between the soft and hard constituent layers. It is expected that the heterogeneous design could be also helpful in improving the deformation compatibility of other nanolayered structures with alternatively stacked soft and hard constituent layers, such as the Cu/Ni system.[3,33,35] The present work on the Cu/Ni system is a first attempt to reveal the deformation mechanism of heterogeneous nanolayered structures by molecular dynamics (MD) simulations. The simulations on heterogenous Cu/Nb and Cu/Zr systems are also in progress and will be reported elsewhere. The simulated heterogeneous Cu/Ni NL sample consists of 2.5 nm and 24 nm bilayers, in which both surfaces of each 24 nm Cu or Ni layer are coated by one 2.5 nm Cu/Ni bilayer. The two values of 2.5 nm and 24 nm are selected to achieve the heterogeneous design and to save computation time. The deformation of a bimodal 2.5 nm–24 nm Cu/Ni sample as well as those of 2.5 nm and 24 nm homogeneous samples was also investigated. The simulations show that, in the homogeneous structure, the dislocations in Cu layers nucleate and glide much earlier than those in Ni layers. It means that the softer Cu layer is much easier to deform, which represents the deformation incompatibility among the Cu and Ni layers. The introduction of the bimodal structure promoted the dislocation activity in Ni layers. Furthermore, in the heterogeneous structure, the dislocation activity in the 24 nm Ni layers is further enhanced and almost occurs synchronously with that in the 24 nm Cu layers.

II. SIMULATION MODEL AND METHOD

We investigated the compression of the layered sample by a large-scale atomic/molecular massively parallel simulator (LAMMPS).[36] The widely used embedded atom method (EAM) potential developed by Daw and Baskes[37] was employed to model the interaction between Cu and Ni atoms in all the Cu/Ni NL samples. The specific values of the EAM potential parameters for Cu and Ni were adopted from Zhou *et al.*[38] The homogeneous NL structure is produced by alternatively stacking Cu and Ni layers with the same thickness (2.5 nm or 24 nm) [Fig. 1(a)], while the bimodal structure is generated by alternatively stacking one 2.5 nm Cu/Ni bilayer and one 24 nm Cu/Ni bilayer [Fig. 1(b)]. Note that the numerals in the above and the following denote the thickness of the Cu or Ni layer, rather than the Cu/Ni bilayer. The new heterogeneous NL structure is formed by adding another 2.5 nm Cu/Ni bilayer in the 24 nm Cu/Ni bilayer interface [Fig. 1(c)]. The lattice orientations of all the Cu and Ni atoms on x, y, and z axes are [112], [$\bar{1}$10], and [$\bar{1}\bar{1}$1], respectively. All the simulated models are constructed by ATOMSK.[39] The above thickness values are for individual layers and are nominal ones. The actual layer thickness can be calculated by $h_{Cu} = N_1\sqrt{3}a_{Cu}$ or $h_{Ni} = N_2\sqrt{3}a_{Ni}$, in which $a_{Cu} = 0.3615$ nm and $a_{Ni} = 0.3520$ nm are, respectively, the lattice constants of Cu and Ni. The actual thicknesses of 2.5 nm Cu and Ni layers are 2.50 nm and 2.44 nm, respectively, while those of 24 nm Cu and Ni layers are 23.79 nm and 23.78 nm, respectively. The dimensions of the simulation cell for all the NL structures are 21.25 nm in the x direction and 19.43 nm in the y direction. Periodic boundary conditions were imposed in all directions. The Polak-Ribiere version of the conjugate gradient algorithm was used in energy minimization. The models were equilibrated in the isothermal-isobaric ensemble (NPT) at 300 K with all the stress components in three directions maintaining zero for 700 ps. After that, the compression was performed under a constant strain rate of -10^9/s along the z direction in the isothermal-isobaric ensemble (NPT), while the other two directions were in stress-free conditions. In addition, the Nose–Hoover thermostat and a barostat are used to control the system temperature and pressure, respectively, with a time step of 1.0 fs. The simulation results are analyzed by using the software OVITO.[40] The number of dislocations of each layer can be obtained by DXA.[41] Since the volume change of each

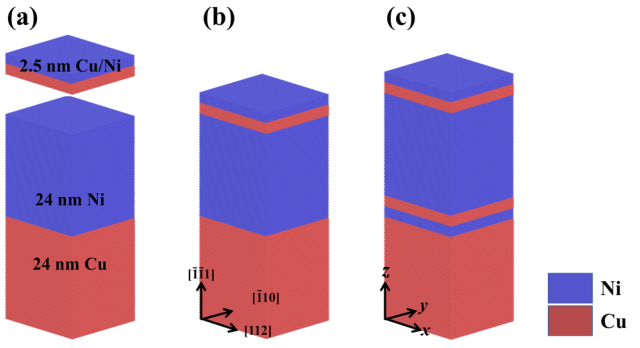

FIG. 1. The computational models for Cu/Ni nanolayered (NL) composites: (a) homogeneous structure with layer thicknesses of 2.5 nm and 24 nm; (b) bimodal structure with alternatively stacked 2.5 nm and 24 nm Cu/Ni bilayers; and (c) heterogeneous structure with one 2.5 nm Cu/Ni bilayer on both sides of each 24 nm Cu and Ni layer. The Cu and Ni atoms are presented by red and blue atoms, respectively.

layer is small due to the small strain applied and the periodic boundary condition, the initial volume of each layer was used to calculate the dislocation density under different strains.

III. RESULTS AND DISCUSSION

After relaxation, all the samples exhibit periodic triangular dislocation networks in the semicoherent Cu/Ni {111} interfaces, which are mainly composed of 1/6⟨112⟩ Shockley partial dislocations, and a few 1/2⟨110⟩ perfect dislocations as well as a small amount of other kinds of dislocations. The interface is divided into two parts by the dislocation networks: one consists of FCC atoms and the other one contains the intrinsic stacking fault (ISF), as shown in Fig. 2(c). This phenomenon has also been observed by Chen *et al.*[39] and Xiang *et al.*[42,43] In addition, there exists a slight difference in the size of networks for NLs with different layer thicknesses. In the following analysis, the FCC and other atoms are deleted in all the models for the sake of a clearer observation of the microstructure.

A. Deformation of homogeneous Cu/Ni nanolayers

Figures 3(a) and 3(b) present the deformation of the 2.5 nm homogeneous Cu/Ni NLs. The results show that there are three deformation stages. In the first stage, the Cu and Ni layers are in the elastic deformation stage, and there is no dislocation in the layers. Then, some semicircular Shockley partial dislocations are nucleated at the nodes of the dislocation network on the side of the Cu layer. There are also some 1/6⟨110⟩ stair-rod dislocations forming near the nodes, but there is still no dislocation in the interior of the layers until a strain of 4.5% [Fig. 3(a)]. In the semicoherent Cu/Ni interface, stress concentration occurs at the node and misfit dislocations as validated by the stress contour in Fig. 2(b), thus giving priority to the nucleation of dislocations at these locations.[44] After the dislocation nucleation at the node of dislocation networks, some dislocations begin to extend from the interface to the Cu layer interior. In this stage, only the Cu layer is subjected to plastic deformation, whereas the Ni layer is still in elastic deformation. Dislocations glide in several {111} slip planes and finally stop at the Cu/Ni interface. The coherent stress and the dislocation network interact with the gliding dislocations, making the semicoherent Cu/Ni {111} interface as an obstacle to dislocation motion.[33] In the third stage, plastic deformation initiates in the Ni layer when dislocations begin to glide in the Ni layer under a sufficiently large strain of 5.9% [Fig. 3(b)]. Now, the whole layered structure reaches the fully plastic deformation stage. The deformation of the 24 nm Cu/Ni NLs is similar to that of the 2.5 nm Cu/Ni layer. The difference lies in the specific strains that correspond to different stages as well as the shape of stacking faults [Figs. 3(c) and 3(d)]. In summary, the plastic deformation of Ni layers in homogeneous structures occurs later than that of Cu layers due to

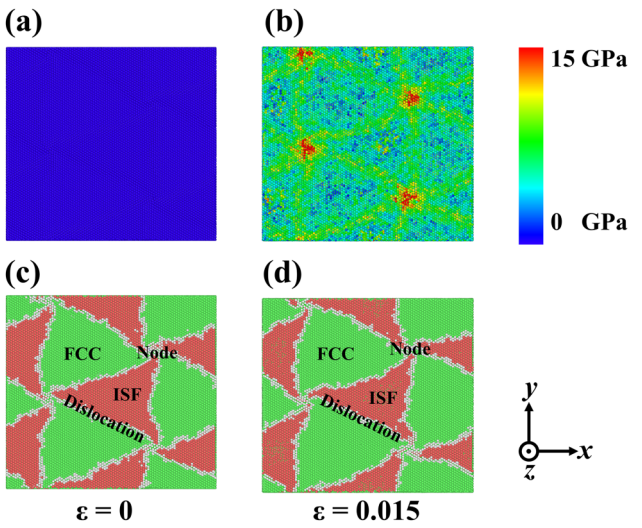

FIG. 2. Stress distribution of the 24 nm Cu–2.5 nm Ni interface in the heterogeneous structure under strains of (a) 0 and (b) 0.015. Dislocation analysis (DXA) results of the same interface under strains of (c) 0 and (d) 0.015. In the dislocation analysis, the atoms are colored to be green for the FCC structure, red for the HCP structure, and white for the other structure.

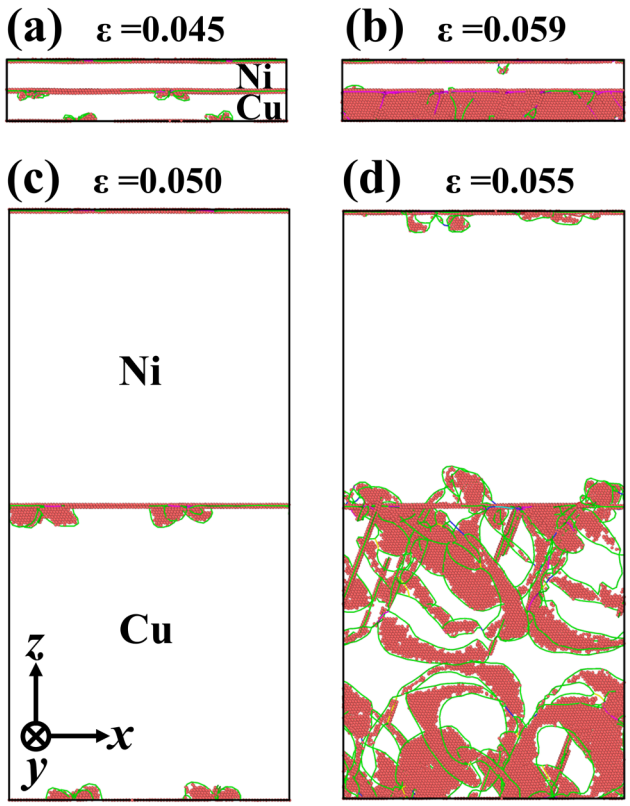

FIG. 3. Deformation of 2.5 nm homogeneous Cu/Ni NLs, (a) ε = 0.045 and (b) ε = 0.059; Deformation of 24 nm homogeneous Cu/Ni NLs, (c) ε = 0.050 and (d) ε = 0.055. Different types of dislocations are represented by lines of different colors, i.e., green, blue, and purple for Shockley partial, perfect, and stair-rod dislocations, respectively.

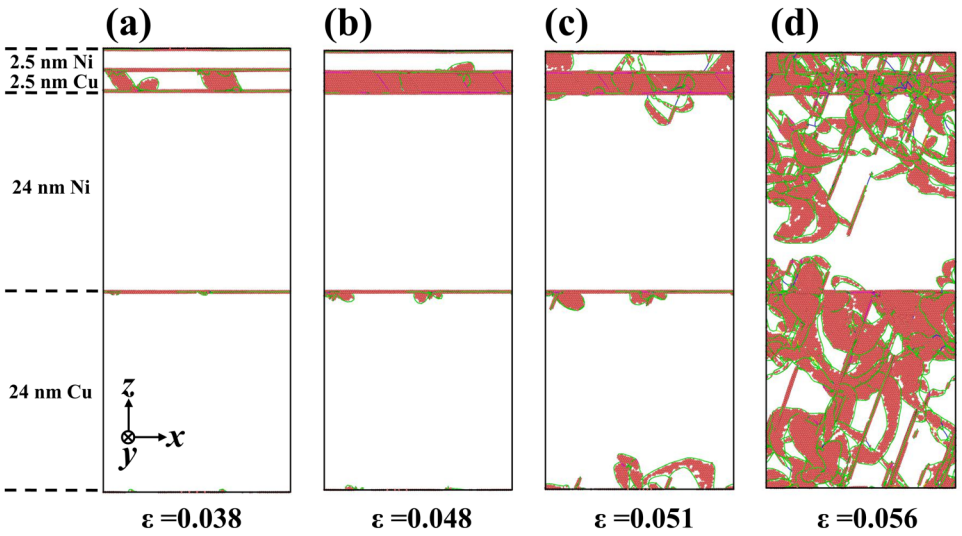

FIG. 4. Deformation of 2.5 nm/24 nm bimodal Cu/Ni NLs.

the higher hardness of the former than that of the latter. The dislocation activities in Ni layers are always much lower than those in Cu layers. The above findings demonstrated the incompatible deformation among the Cu and Ni layers for both thicknesses (2.5 nm and 24 nm).

B. Deformation of bimodal Cu/Ni nanolayers

Figure 4 shows the dislocation evolution of the 2.5 nm/24 nm bimodal Cu/Ni NL structure. The results show that dislocations first nucleate at both sides/interfaces of the 2.5 nm Cu layer and then propagate into the 2.5 nm Cu layer [Fig. 4(a)]. Later, some dislocations are nucleated at the interfaces of the 24 nm Cu layer and some glide in the 2.5 nm Ni layer [Fig. 4(b)]. When dislocations start to nucleate and glide in the 24 nm Ni layers, some dislocations have already extended into the 24 nm Cu layer, as shown in Fig. 4(c). Note that the dislocations in the 24 nm Ni layer first extend from the 2.5 nm Cu–24 nm Ni interface at a strain of 5.1% and then extend from the 24 nm Cu–24 nm Ni interface at a strain below 5.6% [Fig. 4(d)]. This observation differs from that in the 24 nm homogeneous structure, in which dislocations nucleate almost simultaneously in the upper and lower interfaces of the 24 nm Ni layer [Fig. 3(d)]. The findings suggest that the thin 2.5 nm Cu layer promoted the nucleation and multiplication of dislocations in the 24 nm Ni layers. As a result, the dislocation activities in the 24 nm Ni layer of the bimodal structure are more intensive than those of the 24 nm homogeneous structure. For example, dislocations start to occur

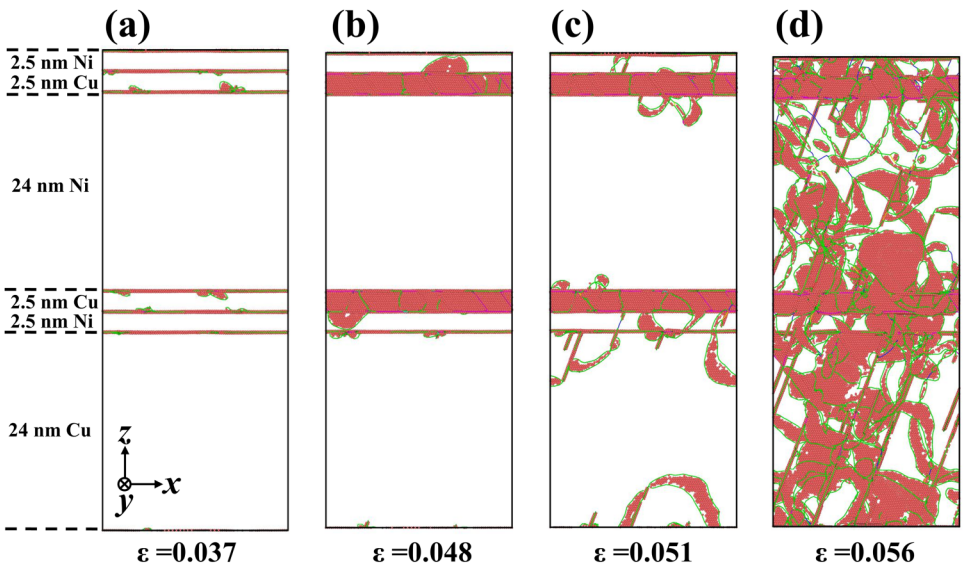

FIG. 5. Deformation of heterogeneous Cu/Ni NLs.

in the 24 nm Ni layer in the bimodal structure at a strain of 5.1%, but dislocations do not occur until a strain of 5.5% in the 24 nm homogeneous structure.

C. Deformation of heterogeneous Cu/Ni NLs

Figure 5 shows that the motion of dislocations in the 24 nm Ni layer of the heterogeneous structure, i.e., 0.037, 0.048, 0.051, and 0.056. Firstly, dislocations nucleate at both interfaces of 2.5 nm Cu layers at a strain of 3.7% [Fig. 5(a)] and then glide into the 2.5 nm Ni layer at a strain of 4.8% [Fig. 5(b)]. Some Shockley partial dislocations are nucleated at the node of dislocation networks of the 2.5 nm Ni–24 nm Cu interface and propagate into the 24 nm Cu layer at a strain of 5.1%. Simultaneously, some dislocations extend from the upper and lower 2.5 nm Cu–24 nm Ni interfaces into the 24 nm Ni layers [Fig. 5(c)]. Note that dislocations already exist in the 24 nm Ni layer of the heterogeneous structure when the strain is 5.1%, but there is no dislocation in that of the 24 nm homogeneous structure until the strain of 5.5%. Figure 5(d) shows that at a strain of 5.6% both the 24 nm Cu and 24 nm Ni layers are full of dislocations, which is not the case of the homogeneous and the bimodal structures. The findings show that the dislocation activity in the 24 nm Ni layer in the heterogeneous structure has been significantly enhanced, and it can reach a level that is comparable to that in the 24 nm Cu layer.

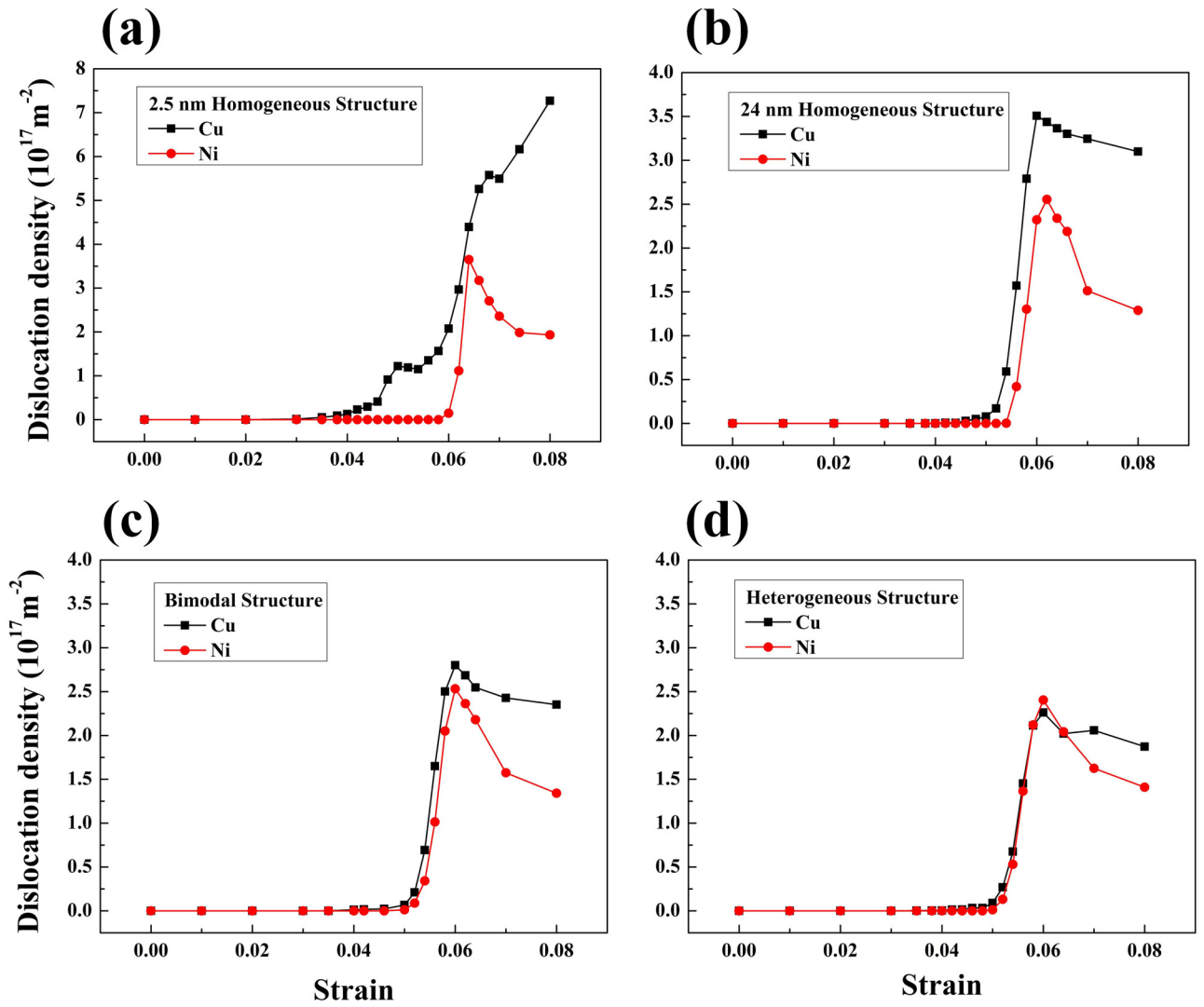

FIG. 6. Variation of the dislocation density in Cu and Ni layers with respect to the applied strain for 2.5 nm (a) and 24 nm (b) homogeneous structures, bimodal structure (c), and heterogeneous structure (d). The dislocation density of 24 nm layers is calculated in the bimodal and the heterogeneous structures.

D. Quantification of the deformation of homogeneous, bimodal, and heterogeneous nanolayers

In order to quantify the dislocation activities of the Cu/Ni NLs, we calculated the dislocation density in the 2.5 nm or 24 nm layers with respect to the applied strain. Figure 6 presents the dislocation density for the homogeneous [Figs. 6(a) and 6(b)], bimodal [Fig. 6(c)], and heterogeneous [Fig. 6(d)] NLs. The results show that the dislocation density in the Cu layer of the 2.5 nm homogeneous Cu/Ni structure starts to be larger than zero at a strain of 3.8% and further increases with the applied strain. However, the dislocation density in the Ni layer remains to be zero until a strain of 6.0%. The Cu and Ni layers have a great difference in dislocation densities, e.g., the density in the former is $7.27 \times 10^{17}\ m^{-2}$, whereas that in the latter is $1.93 \times 10^{17}\ m^{-2}$ at a strain of 8.0% [Fig. 6(a)]. The above phenomenon is also observed in 24 nm homogeneous Cu/Ni NLs, in which the strain corresponding to nonzero dislocation density is 4.6% in the Cu layer and 5.4% in the Ni layer. Under the strain of 8%, the dislocation densities of the Cu and Ni layers are $3.10 \times 10^{17}\ m^{-2}$ and $1.29 \times 10^{17}\ m^{-2}$, respectively. The huge difference in the occurrence of the first dislocation and the dislocation density is a typical indication of the deformation incompatibility among the Cu and Ni layers of the homogeneous structure. As for the bimodal structure, the applied strain at which the dislocation density is no longer zero is 4.0% for the Cu layer and 5.0% for the Ni layer. The dislocation density increases slowly in the Cu layer at the initial stage. Moreover, the dislocation density at a strain of 8.0% is $2.35 \times 10^{17}\ m^{-2}$ in the Cu layer and $1.34 \times 10^{17}\ m^{-2}$ in the Ni layer. Due to the added 2.5 nm Cu/Ni layer, the difference in the dislocation density in Cu and Ni layers becomes smaller.

It is remarkable to note that the dislocation density curves of the 24 nm Cu and the 24 nm Ni layers almost coincide until a strain of 6.4% in the heterogeneous structure [Fig. 6(d)]. Furthermore, the difference in the dislocation density in the Cu and Ni layers is much smaller in the heterogeneous structure than those of the homogenous and bimodal structures. For example, at a strain of 8.0%, the dislocation density difference is $0.46 \times 10^{17}\ m^{-2}$ in the heterogeneous sample, while those for homogeneous and bimodal samples are $1.81 \times 10^{17}\ m^{-2}$ and $1.01 \times 10^{17}\ m^{-2}$, respectively.

In addition, to more clearly show the enhanced dislocation activity in the Ni layer, we defined a parameter $F = (D_{Cu} - D_{Ni})/D_{Cu}$, in which D_x denotes the dislocation density of metal x (=Cu or Ni). The parameter is used to quantify the difference in the dislocation density for Cu and Ni layers. Smaller F suggests better deformation compatibility. The variations of F with respect to the applied strain for homogeneous, bimodal, and heterogeneous structures are shown in Fig. 7. The results show that the new heterogeneous structure has the smallest F as compared to the homogeneous and bimodal structures during almost the whole deformation stage.

The findings show that the two dissimilar materials now can deform synchronously although they have high hardness contrast (2.1 GPa for Cu and 5.5 GPa for Ni[45,46]). That is, the deformation compatibility among the Cu and Ni layers has been significantly enhanced in the new heterogeneous structure. In addition, the values of strain that corresponds to the nonzero dislocation density

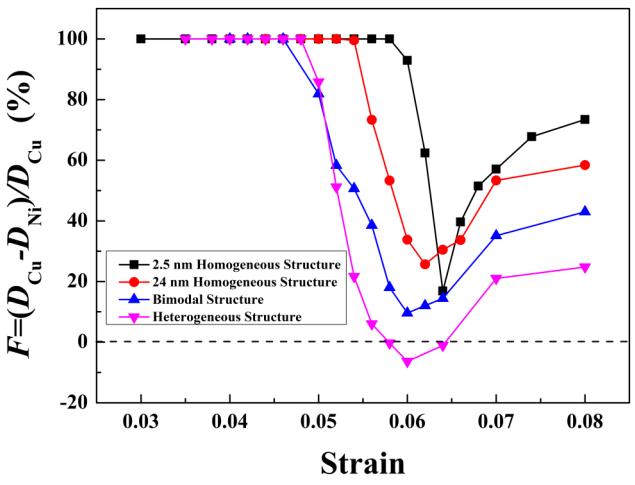

FIG. 7. Variation of F with respect to the applied strain for homogeneous, bimodal, and heterogeneous NLs.

in the 24 nm Ni layer are 0.050 and 0.054 in heterogeneous and 24 nm homogeneous Cu/Ni structures, respectively. This result suggests that the dislocation activities in the 24 nm Ni layer of the heterogeneous structure have been promoted as compared to those of the homogeneous structures. The peak values of dislocation density of the 24 nm Ni layer are $2.55 \times 10^{17}\ m^{-2}$, $2.53 \times 10^{17}\ m^{-2}$, and $2.40 \times 10^{17}\ m^{-2}$ in 24 nm homogeneous, bimodal, and heterogeneous structures, respectively, but those of the 24 nm Cu layer is $3.51 \times 10^{17}\ m^{-2}$, $2.80 \times 10^{17}\ m^{-2}$, and $2.26 \times 10^{17}\ m^{-2}$, respectively. That is, the dislocation density of the 24 nm Cu layer can be tuned to be a level comparable to that of the 24 nm Ni layer by architecting the new heterogeneous nanolayer structure. Thus, the Cu and Ni layers can now deform compatibly.

Next, in order to obtain a comprehensive understanding of the deformation of the heterogeneous nanolayer structures, we replaced the 2.5 nm Cu/Ni bilayers with those having different layer thicknesses, i.e., $t = 1.25$ nm, 5 nm, and 8.8 nm. Here, t denotes the thickness of the Cu or Ni layer. The result for $t = 2.5$ nm is also included for comparison [Fig. 8(b)]. Figure 8(a) shows that the dislocation density is no longer zero in the Cu layer under a strain of 4.6%, but it remains zero in the Ni layer under a strain of 5.2%, which means that the dislocation density curve of the Ni layer still lags that of the Cu layer when t is 1.25 nm. In addition, the dislocation density in the Cu layer is $2.23 \times 10^{17}\ m^{-2}$, and that in the Ni layer is $1.21 \times 10^{17}\ m^{-2}$ under a strain of 8.0%. Figure 8(c) shows that the dislocation density in Cu and Ni layers is almost coincident until a strain of 6.0% when t is 5 nm. However, at a strain of 8.0%, the dislocation densities of Cu and Ni layers are $2.59 \times 10^{17}\ m^{-2}$ and $1.09 \times 10^{17}\ m^{-2}$, respectively, which means that there is still a gap between them. Figure 8(d) shows that the dislocation density curve of the Ni layer lags that of the Cu layer again when t increases to 8.8 nm. The dislocation density remains to be zero until the strain reaches 4.6% for Cu and 5.4% for Ni. Under a strain of 8.0%, the dislocation densities of Cu and Ni layers are

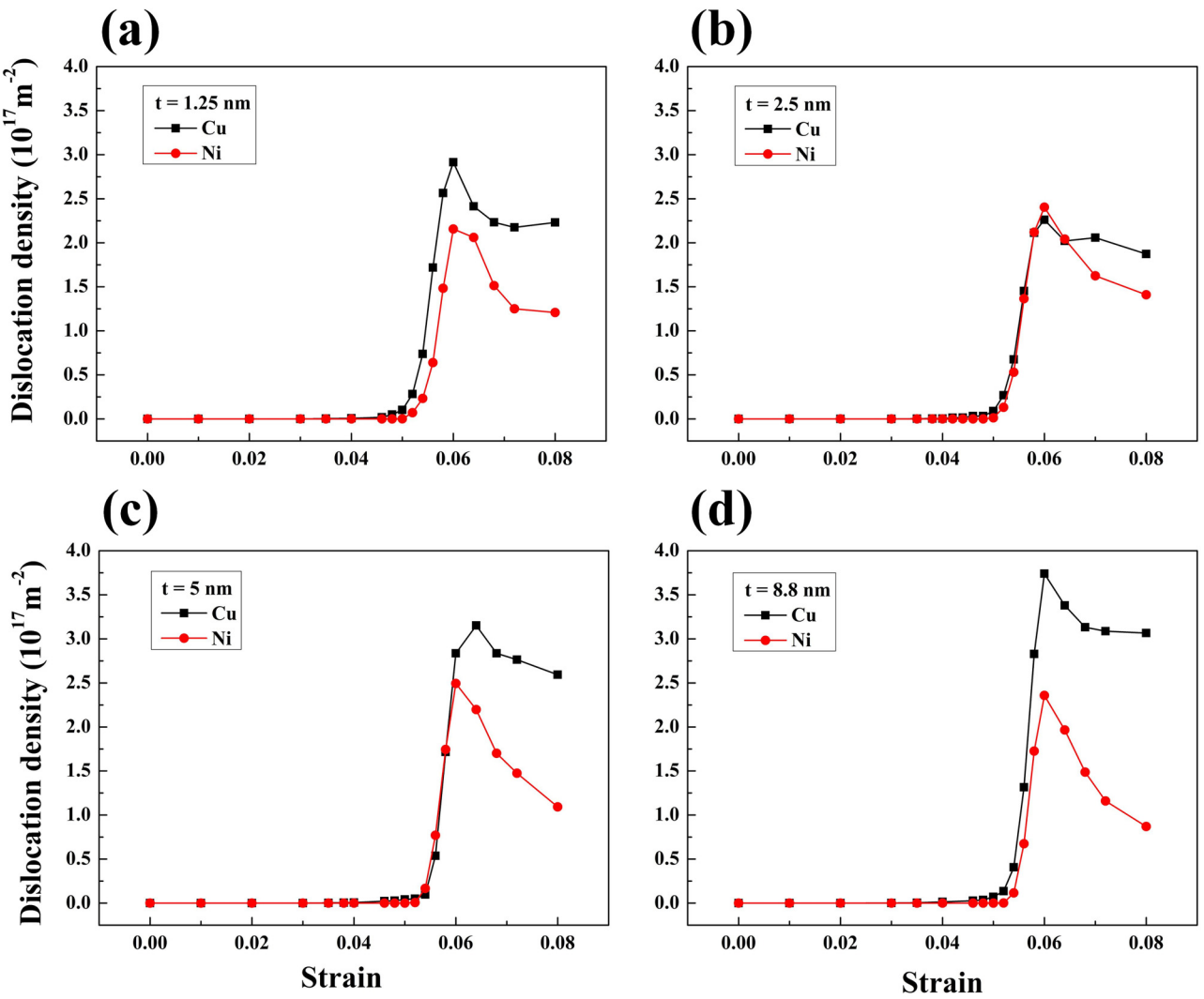

FIG. 8. Variation of the dislocation density in 24 nm Cu and Ni layers with respect to the applied strain for heterogeneous structures with interlayers of various individual thicknesses: t = 1.25 nm (a), 2.5 nm (b), 5 nm (c), and 8.8 nm (d).

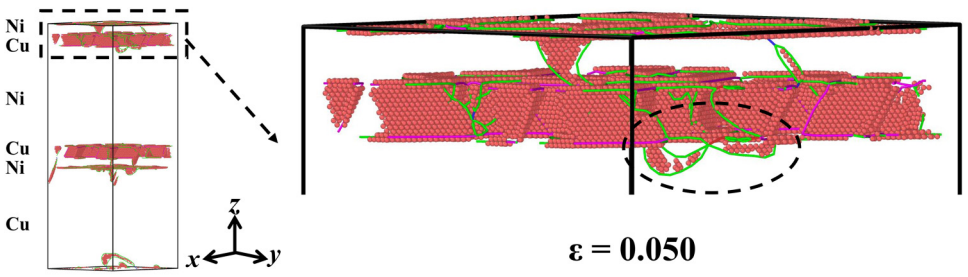

FIG. 9. Microstructure of dislocation nucleation in the heterogeneous structure under a strain of 0.050.

3.07×10^{17} m^{-2} and 0.87×10^{17} m^{-2}, respectively. At a strain of 8.0%, the difference between the dislocation density of Cu and Ni layers is 1.02×10^{17} m^{-2}, 0.46×10^{17} m^{-2}, 1.5×10^{17} m^{-2}, and 2.2×10^{17} m^{-2} when t is 1.25 nm, 2.5 nm, 5 nm, and 8.8 nm, respectively. In addition, the dislocation curves of Cu and Ni layers are the most coincident when t is 2.5 nm. The results show that the best harmony of dislocation motion between Cu and Ni layers in the heterogeneous structure has been achieved in the case of $t = 2.5$ nm. Moreover, the peak value of the dislocation density of the Cu layer is 2.91×10^{17} m^{-2}, 2.26×10^{17} m^{-2}, 3.15×10^{17} m^{-2}, and 3.74×10^{17} m^{-2} when t is 1.25 nm, 2.5 nm, 5 nm, and 8.8 nm, respectively. It is found that the layer thickness of thin layers has a significant effect on the dislocation density of the Cu layer in the heterogeneous structure. Yet, the peak value of the dislocation density of the Ni layer varies from 2.16×10^{17} m^{-2}, 2.40×10^{17} m^{-2}, 2.20×10^{17} m^{-2}, and 2.36×10^{17} m^{-2} for the four thicknesses, showing that the dislocation density of the Ni layer does not change much as t varies.

E. Analysis of the effect of thin layers

Figure 9 shows the microstructure when dislocations first occur in the 24 nm Ni layer under a strain of 0.050 in the heterogeneous structure. These dislocations nucleated at the 2.5 nm Cu–24 nm Ni interface and then slip into the 24 nm Ni layer, as shown in the black dotted line. Therefore, dislocation nucleation is still the main mechanism resulting in the plastic deformation in the 24 nm Ni layer.

The interface has a vital effect on the nanolayered metallic composites.[47] Therefore, the evolution process of the 24 nm Cu–24 nm Ni interface in the 24 nm homogeneous structure and the 2.5 nm Cu–24 nm Ni interface in the heterogeneous structure has been observed, as shown in Fig. 10. As for the 24 nm Cu–24 nm Ni interface in the 24 nm homogeneous structure, there are four nodes (black dotted line) in the dislocation network at the initial stage [Fig. 10(a)]. Some dislocations nucleate at these nodes on the side of the 24 nm Cu layer under a strain of 0.050, resulting in the plastic deformation of the 24 nm Cu layer [Fig. 10(b)]. Dislocations that slip into the 24 nm Ni layer and leads the plastic deformation of this layer nucleate at new nodes (blue dotted line), as shown in Fig. 10(c). There are also four nodes in the dislocation network in the 2.5 nm Cu–24 nm Ni interface in the heterogeneous structure [Fig. 10(d)]. Dislocations nucleate only at these nodes on the side of the 2.5 nm Cu layer [Fig. 10(e)]. Figure 10(f) shows that five new nodes (blue dotted line) have formed under a strain of 0.05. These newly formed nodes are conducive to dislocation nucleation on the side of the 24 nm Ni layer. In addition, dislocations appear in the 2.5 nm Cu layer under a strain of 0.037 [Fig. 5(a)] and then easily approach the 2.5 nm Cu–24 nm Ni interface and interact with the dislocation network. New nodes of the dislocation network form faster in the two interfaces of the 24 nm Ni layer in the heterogeneous structure than that in the 24 nm homogeneous structure due to the interaction. For example, under the same strain of 0.05, there are five new nodes in the upper interface of the 24 nm Ni layer in the heterogeneous structure, but there is no new node in the upper interface of the 24 nm Ni layer in the 24 nm homogeneous structure. Even under a strain of 0.054, there are only four new nodes in that of the 24 nm homogeneous structure. The early appearance of new nodes in the interfaces of the 24 nm

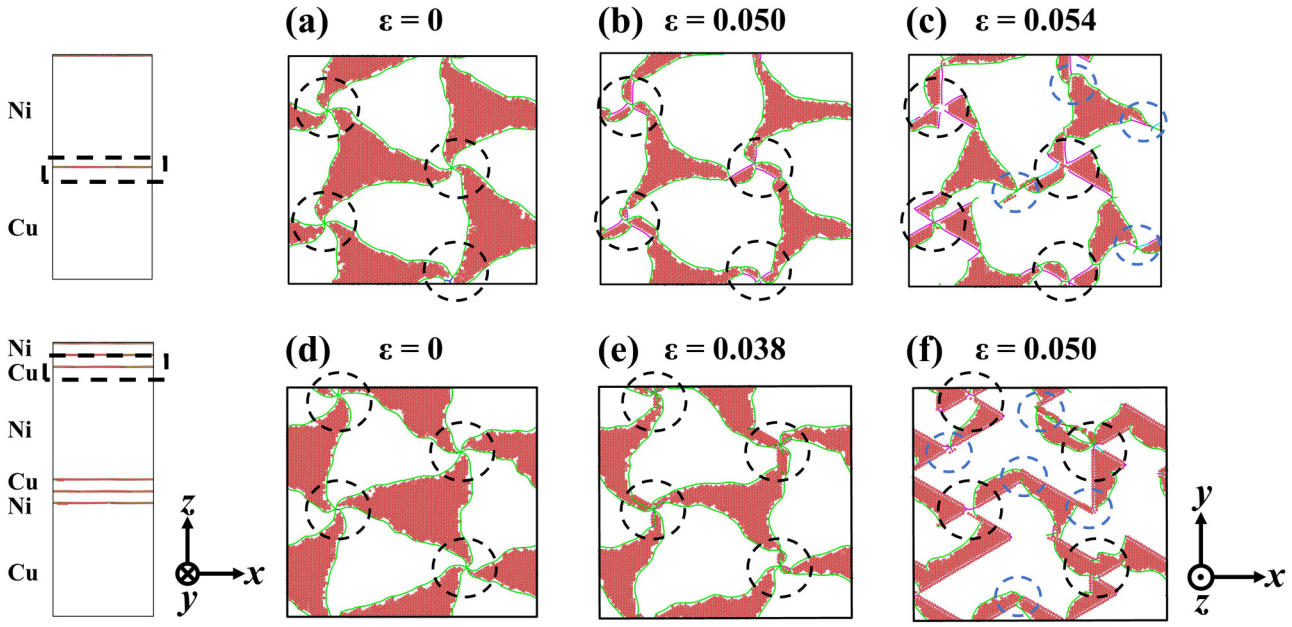

FIG. 10. Dislocation network evolution of the 24 nm Cu–24 nm Ni interface in the 24 nm homogeneous structure, (a) ε = 0, (b) ε = 0.050, and (c) ε = 0.054; Dislocation network evolution of the 2.5 nm Cu–24 nm Ni interface in the heterogeneous structure, (a) ε = 0, (b) ε = 0.038, and (c) ε = 0.050.

Ni layer promotes the dislocation nucleation in the 24 nm Ni layer, making its dislocation activity approach the level of that in the 24 nm Cu layer. Therefore, the deformation compatibility between 24 nm Cu and Ni layers in the heterogeneous structure has been improved.

IV. CONCLUSIONS

The deformations of homogeneous, bimodal, and heterogeneous structures during compression have been studied using molecular dynamics simulations. For the homogeneous layers, our simulations show that the plastic deformation first takes place in the Cu layer and then in the Ni layer, which is a marked sign of deformation incompatibility. As for the bimodal structure, the added 2.5 nm Cu/Ni layer effectively promotes the dislocation activity of the 24 nm Ni layer and lowers the dislocation density of the 24 nm Cu layer to some extent. Therefore, the difference of the dislocation activity between 24 nm Cu and Ni layers becomes smaller. In addition, the deformation compatibility in the heterogeneous structure has been markedly improved. In the heterogeneous structure, both the upper and lower adjacent layers of the 24 nm Ni layer are 2.5 nm Cu/Ni layers that can quicken the evolution of the 2.5 nm Cu–24 nm Ni interface and obtain more new nodes in the dislocation network to promote the dislocation nucleation in the 24 nm Ni layer. On the other hand, the added thin Cu/Ni layers can lower the dislocation density of the 24 nm Cu layer to the level of the 24 nm Ni layer. It makes the dislocation density curves of Cu and Ni layers to be consistent, which also reflects the concordant dislocation activity between Cu and Ni layers. Moreover, the optimal deformation compatibility between 24 nm Cu and Ni layers in the heterogeneous structure occurs when the layer thickness of the thin layer is 2.5 nm. In this way, the deformation compatibility between two materials with obvious mechanical contrast can be significantly improved.

ACKNOWLEDGMENTS

The authors appreciate the financial support from the National Key R&D Program of China (Grant No. 2017YFA0204402), the National Natural Science Foundation of China (NSFC) (Grant No. 11872380), the Natural Science Foundation of Hunan Province under Grant No. 2019JJ50750, the Project of State Key Laboratory of High Performance Complex Manufacturing, Central South University (No. ZZYJKT2018-05), the Opening fund of State Key Laboratory of Nonlinear Mechanics, China, and the start-up fund from Central South University, China.

REFERENCES

[1]M. R. Stoudt, R. E. Ricker, and R. C. Cammarata, Int. J. Fatigue **23**, 215 (2001).
[2]X. Y. Zhu, X. J. Liu, R. L. Zong, F. Zeng, and F. Pan, Mater. Sci. Eng. A **527**, 1243 (2010).
[3]Y. Liu, D. Bufford, H. Wang, C. Sun, and X. Zhang, Acta Mater. **59**, 1924 (2011).
[4]P.-H. Sung, C.-D. Wu, and T.-H. Fang, Comput. Mater. Sci. **56**, 43 (2012).
[5]X. L. Zhou and C. Q. Chen, Comput. Mater. Sci. **101**, 194 (2015).
[6]P. E. Specht, T. P. Weihs, and N. N. Thadhani, J. Appl. Phys. **121**, 015110 (2017).
[7]M. R. An, H. Y. Song, Q. Deng, M. J. Su, and Y. M. Liu, J. Appl. Phys. **125**, 165307 (2019).
[8]M. Jain, N. Velisavljevic, J. K. Baldwin, M. Knezevic, N. A. Mara, I. J. Beyerlein, and S. Pathak, J. Appl. Phys. **126**, 025302 (2019).
[9]A. Misra, M. Verdier, Y. C. Lu, H. Kung, T. E. Mitchell, M. Nastasi, and J. D. Embury, Scr. Mater. **39**, 555 (1998).
[10]J. Mckeown, A. Misra, H. Kung, R. G. Hoagland, and M. Nastasi, Scr. Mater. **46**, 593 (2002).
[11]A. Misra, M. J. Demkowicz, J. Wang, and R. G. Hoagland, JOM **60**, 39 (2008).
[12]J. J. Niu, J. Y. Zhang, G. Liu, P. Zhang, S. Y. Lei, G. J. Zhang, and J. Sun, Acta Mater. **60**, 3677 (2012).
[13]J. Y. Zhang, S. Lei, Y. Liu, J. J. Niu, Y. Chen, G. Liu, X. Zhang, and J. Sun, Acta Mater. **60**, 1610 (2012).
[14]P. M. Anderson and C. Li, Nanostruct. Mater. **5**, 349 (1995).
[15]A. Misra, J. P. Hirth, and H. Kung, Philos. Mag. A **82**, 2935 (2002).
[16]A. Misra, J. P. Hirth, and R. G. Hoagland, Acta Mater. **53**, 4817 (2005).
[17]N. Abdolrahim, H. M. Zbib, and D. F. Bahr, Int. J. Plast. **52**, 33 (2014).
[18]Y. Y. Lu, R. Kotoka, J. P. Ligda, B. B. Cao, S. N. Yarmolenko, B. E. Schuster, and Q. Wei, Acta Mater. **63**, 216 (2014).
[19]L. Lu, C. Huang, W. Pi, H. Xiang, F. Gao, T. Fu, and X. Peng, Comput. Mater. Sci. **143**, 63 (2018).
[20]W. Yang, G. Ayoub, I. Salehinia, B. Mansoor, and H. Zbib, Comput. Mater. Sci. **154**, 488 (2018).
[21]H. Huang and F. Spaepen, Acta Mater. **48**, 3261 (2000).
[22]N. A. Mara, D. Bhattacharyya, R. G. Hoagland, and A. Misra, Scr. Mater. **58**, 874 (2008).
[23]I. J. Beyerlein, N. A. Mara, J. Wang, J. S. Carpenter, S. J. Zheng, W. Z. Han, R. F. Zhang, K. Kang, T. Nizolek, and T. M. Pollock, JOM **64**, 1192 (2012).
[24]G. P. Zhang, Y. Liu, W. Wang, and J. Tan, Appl. Phys. Lett. **88**, 013105 (2006).
[25]Y. P. Li, X. F. Zhu, G. P. Zhang, J. Tan, W. Wang, and B. Wu, Philos. Mag. **90**, 3049 (2010).
[26]Y. P. Li, X. F. Zhu, J. Tan, B. Wu, W. Wang, and G. P. Zhang, J. Mater. Res. **24**, 728 (2009).
[27]J. Y. Zhang, S. Lei, J. Niu, Y. Liu, G. Liu, X. Zhang, and J. Sun, Acta Mater. **60**, 4054 (2012).
[28]J. Y. Zhang, G. Liu, S. Y. Lei, J. J. Niu, and J. Sun, Acta Mater. **60**, 7183 (2012).
[29]A. Misra and R. G. Hoagland, J. Mater. Sci. **42**, 1765 (2007).
[30]Y. Wang, J. Li, A. V. Hamza, and T. W. Barbee, Proc. Natl. Acad. Sci. U.S.A. **104**, 11155 (2007).
[31]T. A. Wynn, D. Bhattacharyya, D. L. Hammon, A. Misra, and N. A. Mara, Mater. Sci. Eng. A **564**, 213 (2013).
[32]J. Li, W. Lu, S. Zhang, and D. Raabe, Sci. Rep. **7**, 11371 (2017).
[33]R. G. Hoagland, T. E. Mitchell, J. P. Hirth, and H. Kung, Philos. Mag. A **82**, 643 (2002).
[34]J. Y. Zhang, G. Liu, and J. Sun, Acta Mater. **61**, 6868 (2013).
[35]M. D. Gram, J. S. Carpenter, and P. M. Anderson, Acta Mater. **92**, 255 (2015).
[36]S. Plimpton, J. Comput. Phys. **117**, 1 (1995).
[37]S. M. Foiles, M. I. Baskes, and M. S. Daw, Phys. Rev. B **37**, 10378 (1988).
[38]X. W. Zhou, R. A. Johnson, and H. N. G. Wadley, Phys. Rev. B **69**, 144113 (2004).
[39]P. Hirel, Comput. Phys. Commun. **197**, 212 (2015).
[40]A. Stukowski, Modell. Simul. Mater. Sci. Eng. **18**, 015012 (2010).
[41]A. Stukowski, V. V. Bulatov, and A. Arsenlis, Modell. Simul. Mater. Sci. Eng. **20**, 085007 (2012).
[42]G. Chen, C. Wang, and P. Zhang, Comput. Mater. Sci. **131**, 21 (2017).
[43]M. Xiang, Y. Liao, K. Wang, and G. Lu, and J. Chen, Int. J. Plast. **103**, 23 (2018).
[44]S. Shao, J. Wang, I. J. Beyerlein, and A. Misra, Acta Mater. **98**, 206 (2015).
[45]S. P. Wen, R. L. Zong, F. Zeng, Y. Guo, and F. Pan, Acta Mater. **55**, 345 (2007).
[46]S. P. Wen, R. L. Zong, F. Zeng, S. Guo, and F. Pan, Appl. Surf. Sci. **255**, 4558 (2009).
[47]F. Yin, Y. Zhao, S. Yu, and W. Pang, J. Appl. Phys. **125**, 025112 (2019).